sciendo

POLISH MARITIME RESEARCH 2 (106) 2020 Vol. 27; pp. 107-119
10.2478/pomr-2020-0032

DESIGN ANALYSIS OF HYBRID GAS TURBINE–FUEL CELL POWER PLANT IN STATIONARY AND MARINE APPLICATIONS

Tomasz Kwaśniewski
Marian Piwowarski
Gdańsk University of Technology, Poland

ABSTRACT

The paper concerns the design analysis of a hybrid gas turbine power plant with a fuel cell (stack). The aim of this work was to find the most favourable variant of the medium capacity (approximately 10 MW) hybrid system. In the article, computational analysis of two variants of such a system was carried out. The analysis made it possible to calculate the capacity, efficiency of both variants and other parameters like the flue gas temperature. The paper shows that such hybrid cycles can theoretically achieve extremely high efficiency over 60%. The most favourable one was selected for further detailed thermodynamic and flow calculations. As part of this calculation, a multi-stage axial compressor, axial turbine, fuel cell (stack) and regenerative heat exchanger were designed. Then an analysis of the profitability of the installation was carried out, which showed that the current state of development of this technology and its cost make the project unprofitable. For several years, however, tendencies of decreasing prices of fuel cells have been observed, which allows the conclusion that hybrid systems will start to be created. This may apply to both stationary and marine applications. Hybrid solutions related to electrical power transmission, including fuel cells, are real and very promising for smaller car ferries and shorter ferry routes.

Keywords: gas turbine cycles, hybrid cycles, design of gas turbines, fuel cells

INTRODUCTION

CURRENT CONDITION OF POLISH POWER INDUSTRY

Nowadays, the Polish power industry is facing serious challenges related with various technological and economic aspects (power mix modification, for instance). Bearing in mind the EU regulations that Poland agreed to observe, the structure of primary fuel consumption should be radically changed. The restrictions to be introduced should aim at a considerable reduction in emissions of toxic compounds to the atmosphere, including carbon monoxide and dioxide, sulphur oxides, and nitrogen oxides, which accompany the combustion of fossil fuels. Bituminous coal and lignite are well-known to constitute the basis of the Polish power industry (in 2016, 81% of electricity was produced in coal-fired power plants [22]). This situation can be changed in two ways. The first option consists in reducing the coal percentage in the domestic power mix, which can be achieved by decreasing electricity production in conventional power plants and/or by increasing its production in other, more environmentally friendly power units. This may refer to the utilisation of other working media [1, 8, 15, 21, 23] and power plants with microturbines [33, 34, 35]. The other option is the use of expensive systems for carbon dioxide capture and storage (CCS). At present, (March, 2019) the scenario which assumes a considerable reduction of electricity production in coal-fired power plants does not appear realistic. At the same time, the CCS systems are currently economically unprofitable, due to the still relatively low charges for carbon dioxide emission to the atmosphere. The outline plan of

domestic power industry development is presented in the document published by the Ministry of Energy and entitled "Energy Policy for Poland until 2040" (PEP2040) [17]. It results from this document that, in the more distant future, building electric power plants with CO_2 emission close or exactly equal to zero seems inevitable. A priority will be intensive development of renewable energy sources (RES), but also the development of natural gas-fired plants [9, 10]. PEP2040 includes the information that these plants will provide control services for the National Power System (NPS). Moreover, it is indicated that natural gas, as a fuel which emits smaller amounts of toxic substances than coal, is expected to be the source of power in the interim period on the way to the low-emission RES-based power generation technology. This direction of development seems advisable, but some experts have provided evidence that the role of natural gas has been underestimated [24], as in the next 10–15 years a number of coal-fired blocks will need to be switched off due to their advanced age, and in this situation natural gas can be a good replacement for coal. Moreover, onshore wind power plants will be successively dismantled, and new ones will not be built due to unfavourable legal regulations [27]. Offshore wind power energy is planned to be utilised in Poland in the next 10–20 years, but this energy source is well-known to be uncontrollable. At the same time, building a nuclear power plant is still questionable. In the context of the above problems of the NPS, it is advisable to look for modern electricity sources. A good example of such an unconventional approach is a hybrid system being a combination of fuel cell with gas turbine.

HYBRID GAS TURBINE–FUEL CELL OPPORTUNITIES IN THE MARINE FIELD

Ships and vessels are responsible for 15% of the nitrogen oxide global emission and 6% of the carbon dioxide. What is more, ships and vessels are accountable for about 5–10% of acid rain in coastal regions [30, 31]. This has resulted in the imposition of international standards since 2015 for fuel with a maximum sulphur content below 0.1%. This forces vessels on the Baltic to use a fuel other than heavy fuel. This is an opportunity for a new type of vessel, e.g. hybrid drives with gas-powered units, such as LNG or fuel cells. DNV-GL experts observe that "zero-emission" technologies are becoming more and more popular in the marine world, together with the decision to implement a global sulphur emission reduction in 2020 and to include the North Sea and the Baltic Sea in the list of nitrous oxide (NOX) emission control areas. Natural gas (consisting of 70–90% methane) does not contain sulphur, but it sometimes contains a significant amount of nitrogen, but there are well known denitrogenation methods. This is why natural gas is often highlighted as the cleanest fossil fuel. Moreover, it is technically possible to feed a fuel cell with natural gas. It should be emphasised that the "zero emission" technology uses fuel cells as the main drive and source of energy in shipping. Direct conversion provides an electrical efficiency of up to 60%, depending on the type of fuel cells and the fuel used. Fuel cells offer a high potential to reduce emissions to air. An assessment of the potential and limitations of this technology was carried out on ro-pax vessels, as a result of which nearly 150 scenarios were examined, and additional risk mitigation measures were recommended for 100 of these with respect to operational and human safety. Intensive research related to fuel cell technology has been carried out worldwide in more than 20 projects. Different fuels and types of fuel cells are being examined. The capacity of each project is between 12 kW and 2.5 MW. Projects such as RiverCell by the German consortium "e4ships" include feasibility studies and the future role of fuel cells (main or auxiliary power supply). Fuel cells are quiet, efficient and do not cause noticeable vibrations.

Unfortunately, fuel cell technology is not without its disadvantages. The most significant problem is related to the fuel itself. Hydrogen – commonly used to feed the fuel cell – does not appear in a molecular form in nature. The methods of its production, although well-developed technologically, are still rather expensive [5, 31]. What is more, hydrogen is an extremely difficult gas to store, which seriously limits further development of hydrogen technologies. Because of its low density (0.07 g/cm^3 at standard temperature and pressure), a hydrogen gas tank that contains a store of energy equivalent to a traditional fuel tank would be more than 3,000 times bigger. When choosing an appropriate storage system for marine application, the following aspects must be taken into consideration: cost, energy density and desired storage period. In the context of these requirements, the storage of liquefied hydrogen may appear to be the best storage option.

The only gas that can be used onboard as accepted by classification societies is natural gas. The first rules for using fuel cells onboard were developed by Germanischer Lloyd (GL) in cooperation with The International Gas Code (IGC) in 2003. Other classification societies like Bureau Veritas (BV) and Det Norske Veritas (DNV) are working on a comprehensive set of guidelines for the use of fuel stacks and hydrogen fuel onboard commercial ships [32, 36]. The guidelines produced by BV are now being tested on pilot projects like the Hydrogen-Power Hybrid Electric Harbour Tug [30].

The marine environment would be challenging for fuel cells. There are certain requirements for the technology which are not so important in stationary applications: high power density related to weight and size, tolerance to salt air, quick start and load responding characteristics. Despite the technical performance of fuel cells, the ability to use commercially available fossil fuel with low sulphur content instead of pure hydrogen is another challenge of the fuel cell's application in the maritime field. Therefore, fuel cells have also been developed which are fed with other fuels, such as methanol or methane.

PRINCIPLE OF FUEL CELL OPERATION

The fuel cell is a device which performs the electrochemical conversion of chemical energy stored in the fuel into electricity. Its major advantage is a shorter conversion chain

from primary to final energy than that in the conventional thermal power plant (Fig. 1, Fig. 2). This, theoretically at least, results in higher efficiency of the fuel cell.

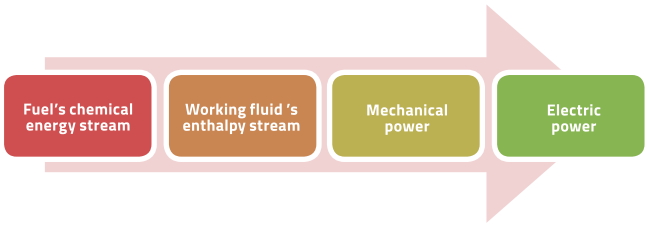

Fig. 1. Energy transformation chain in a typical thermal power plant (useful forms of energy)

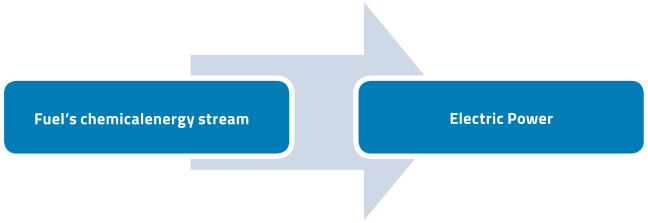

Fig. 2. A chain of energy transformations taking place in a fuel cell

The fuel cell utilises the tendency of H_2 and O_2 molecules to reach the state of the lowest possible energy, i.e. when they are bound in the water molecule H_2O. This tendency can be presented as two electrochemical half-reactions as in Eqs. (1) and (2) [20]:

$$2H_2 \leftrightarrows 4H^+ + 4e^- \quad (1)$$

$$O_2 + 4H^+ + 4e^- \leftrightarrows 2H_2O \quad (2)$$

Adding up these two equations gives the reaction of hydrogen combustion in oxygen, with pure water as a final product. That is why, theoretically, the fuel cell is considered a source of electricity which does not emit toxic substances, such as the carbon oxides CO and CO_2, and sulphur oxides. At idle, a single fuel cell can generate a voltage that rarely exceeds 1 V [20]. In operating (load) conditions, this voltage is even lower and depends on the temperature and current density. It cannot be used directly for supplying conventional receivers; therefore, fuel cells are connected in sets called stacks. The low voltage generated by the fuel cell provides a challenge for the material of electrodes which need to be very good electric conductors. The next technological challenge faced by fuel stack designers is the small rate of reactions taking place on the electrodes, which leads to low values of the electric current flowing in them. The acceleration of these reactions can be obtained in a number of ways (which are frequently executed simultaneously), such as: increasing the working temperature, increasing the working pressure, using catalysers and increasing the surface area of the electrodes (by using porous materials). Fuel cells can be classified in different ways, for instance with respect to the type of electrolyte or fuel, or the working temperature [2]. The most popular polymer fuel cells usually work at temperatures below 120°C. The fuel cell is assumed to be of the high-temperature type when its working temperature exceeds 550°C. This group includes Molten Carbonate Fuel Cells (MCFC) and Solid Oxide Fuel Cells (SOFC). The high temperature of the working medium makes it possible for these fuel cells to cooperate with other power systems, such as gas or steam turbines. The high-temperature fuel cells can also be used in combined heat and power (CHP) systems. Both the abovementioned types of fuel cells are fed with hydrogen, and their high working temperature provides an opportunity for hydrocarbon conversion to molecular hydrogen in the fuel cell or its vicinity. This conversion, known as steam reforming, takes place at temperatures ranging from 700 to 1100°C in the presence of a catalyser and consists in acting with steam on natural gas, for instance. The products of this reaction are hydrogen and carbon monoxide and dioxide.

THEORY OF HYBRID SYSTEM

The idea of a hybrid system is to link thermodynamically a gas turbine system with a fuel cell (stack), with the latter device being the upper heat source for the turbine set. Various methods of linking these two systems are known. Basically, a distinction is made between indirect and direct systems. The former type is characterised by the lack of coupling between the working pressure in the fuel cell stack and that at the gas turbine set exit. The medium is first compressed in the gas turbine set and then heated by the exhaust gas leaving the fuel cell stack. Finally, the medium expands in the gas turbine. In the latter type, on the other hand, the stack pressure depends on that generated by the compressor being part of the gas turbine set, and the heat and mass transfer takes place between the subsystems. In both variants, a combustion chamber may be used, and in those cases, it is most frequently situated directly in front of the turbine. Its role is to increase the inlet temperature of the medium and to burn flammable substances still remaining in the exhaust gas. There have been a number of studies on both types of hybrid systems based on MCFC and SOFC fuel cells. The first attempt to use a hybrid design was made in 2000, when Siemens Westinghouse developed a system with SOFC of 200 kW in power and 50% in efficiency. Unfortunately, there is no data available in the internet on the investigations performed and their final conclusions. What is known is that the system was in operation for about 2900 hours without serious failure [4]. Promising results have been published by Japanese researchers [18]. They built a system of 200 kW in electric power which was continuously in operation for 4000 h, at maximum efficiency of 50.2%. The most recent 250 kW installation, put into operation in 2017, works for Toyota, a Japanese car manufacturer. Its efficiency is estimated to be approximately 55%, and can be additionally increased by 10 percentage points by applying combined heat and power production. The centre of the system is the SOFC fuel cell stack in a tubular arrangement, which means that a single fuel cell has the shape of a tube inside which the fuel flows, and its outside is washed by air. This is a direct system, in which the pressure is generated by a radial compressor that is part of a single-shaft gas turbine set. The working medium flow direction in the turbine and the compressor is radial.

This installation shows that the hybrid technology is already so mature that it can be introduced on a large scale [25]. However, there is still a lack of significant applications of gas turbine–fuel cell hybrid systems in the maritime field (even on a small scale).

MATHEMATICAL ANALYSIS OF HYBRID SYSTEM CYCLES

FUEL CELL STACK

In this article, the hybrid system is presented in two variants: indirect and direct, for an assumed power of the fuel cell stack. The system is optimised to maximise the power of the attached gas turbine set, and thus the power of the entire hybrid system. The list of adopted assumptions is collated in Table 1.

Tab. 1. Assumptions for the analysis of the hybrid system

Quantity	Symbol [unit]	Value
Electric power of the stack[1]	$N_{el,FC}$ [kW]	10000
Dry air composition (molar shares) [18]	N2/O2/Ar [%/%/%]	78.12/20.96/0.92
Air temperature[1]	t_{pow} [°C]	20
Barometric pressure [6]	p_{bar} [kPa]	101.3
Air humidity [6]	φ [%]	60
Fuel type[1]	–	methane
Degree of fuel utilisation by the stack[1]	U_f [%]	85
Heat recovery efficiency[1]	σ_{rek} [–]	0.75
[1] Arbitrarily chosen		

An assumption has been made that the system is fed with methane, so the integral part of the fuel cell stack is the reformer. Consequently, part of the heat generated by the stack is used in a series of chemical reactions which convert methane to hydrogen and carbon dioxide and monoxide, as in Eqs. (3) and (4).

$$CH_4 + 2H_2O \longrightarrow 4H_2 + CO_2 \tag{3}$$

$$H_2 + CO_2 \leftrightarrows CO + H_2O \tag{4}$$

These reactions take place simultaneously. As can be seen, the latter reaction leads to the decrease of the amount of hydrogen in the reformate until the equilibrium state is reached between concentrations of individual compounds (their exact values depend on temperature and pressure).

The gases leaving the fuel cell contain the following chemical compounds: hydrogen, carbon dioxide, carbon oxide, and steam, as calculated in [26]. This information on the chemical composition makes it possible to assess the condition and parameters (calorific value, temperature, specific enthalpy) of the working medium. From the point of view of the user, the most important working parameters of the fuel cell are its voltage and current. The current is the quantity which results from the fuel cell load and can be controlled. By contrast, the voltage is the resultant of different aspects, such as the working pressure, specific resistance of electrodes, working temperature, etc. [26, 30]. The quantities assumed as variables are current density *i* and stack pressure *P*. An individual analysis of the fuel cell stack has revealed that increasing the pressure leads to efficiency increase, but the energy expenditure in the blower drive more than consumes the profit resulting from the pressure increase (Fig. 3). On the other hand, increasing the blower pressure ratio increases the stack power generated per unit area (power density, Fig. 4). As a consequence, the fuel cell stack designer faces a conflicting problem of which criterion to choose: efficiency maximisation (lower costs of fuel), or maximisation of the working area of the fuel cell stack (lower construction costs).

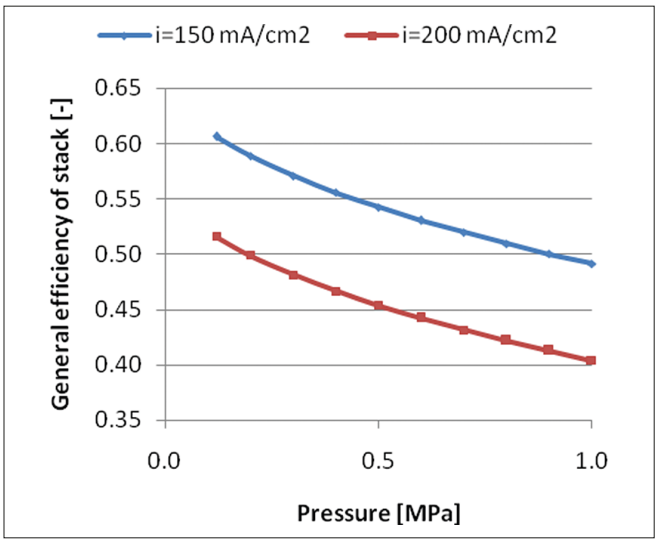

Fig. 3. Influence of pressure and current density on the overall efficiency of the fuel stack

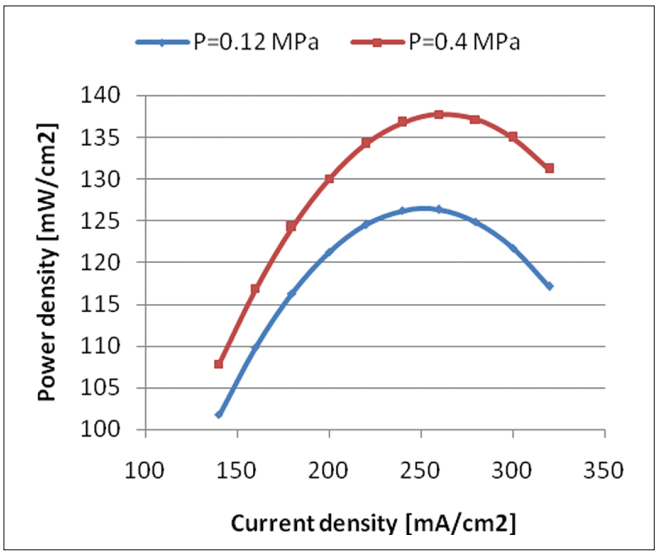

Fig. 4. Influence of current and pressure density on cell power density

INDIRECT HYBRID SYSTEM

In the indirect variant (Fig. 5), the hybrid system is equipped with an after-combustion chamber, in which the amounts of hydrogen remaining after the reaction in the fuel cell stack are combusted. The advantage of this variant is higher reliability, compared to the direct variant, as possible switch-off (failure) of the gas turbine set does not stop the operation of the fuel cell stack. Then, the working pressure of each subsystem can be optimised individually. What is more, the working medium in the gas turbine system is air, which makes the turbine much less subject to corrosion than when operating with exhaust gas as the expanding medium.

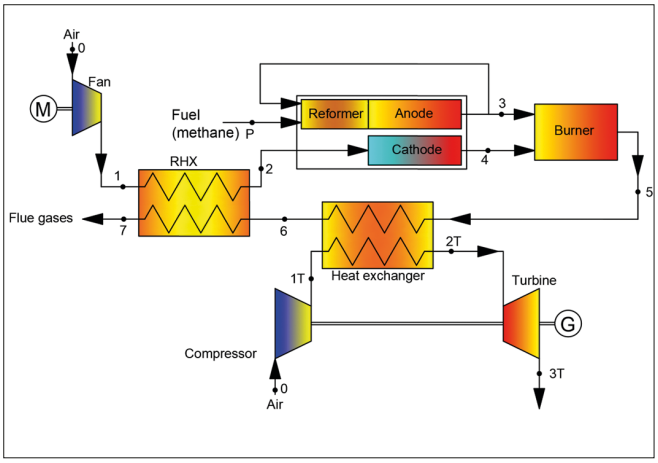

Fig. 5. Indirect hybrid system (RHX – Regenerative Heat Exchanger)

The starting point for calculating the amount of fuel consumed by the stack is the equation of the chemical reaction taking place on the fuel cell anode (Eq. (5)).

$$2H_2 \longrightarrow 4H^+ + 4e^- \tag{5}$$

The above formula says that one mole of hydrogen can produce 2 moles of electrons. One mole of electrons has the charge of 96485 C (the Faraday constant [26]). This makes it possible to calculate the number of moles per unit electric charge (Eq. (6)), and then the mass of hydrogen per unit charge (Eq. (7)).

$$n_{H2} = 1A \cdot \frac{1\frac{C}{s}}{1A} \cdot \frac{1e^-}{96485C} \cdot \frac{1molH_2}{2e^-} = 5{,}18 \cdot 10^{-6}\,\frac{molH_2}{A \cdot s} \tag{6}$$

$$m_{H2} = n_{H2} \cdot M_{H2} = 5{,}18 \cdot 10^{-6}\,\frac{molH_2}{A \cdot s} \cdot 2{,}0158\,\frac{g}{molH_2} = 1{,}04 \cdot 10^{-8}\,\frac{kgH_2}{A \cdot s} \tag{7}$$

The set of assumptions needed for performing the analysis is collated in Table 2. Having assumed the fuel cell power and current density, the fuel cell working area $S_{cał}$ (Eq. (8)) and the expected fuel consumption m_{H2} (Eq. (9)) are calculated.

$$S_{cał} = \frac{N_{FC,netto}}{i \cdot U} \tag{8}$$

$$\dot{m}_{H2} = m_{H2} \cdot i \cdot S_{cał} \tag{9}$$

Tab. 2. Assumptions for the analysis of an indirect hybrid system

Quantity	Symbol [unit]	Value
Electric power of the stack[1]	$N_{FC,netto}$ [kW]	10000
Pressure after the fan[1]	P_1 [MPa]	0.12
The temperature of the medium before the turbine[1]	t_{2T} [°C]	900
Mechanical efficiency of the gas turbine set [7]	$\eta_{mech,TG}$ [%]	99
Isentropic efficiency of the turbine [7]	$\eta_{i,T}$ [%]	88
Isentropic efficiency of the compressor [7]	$\eta_{i,S}$ [%]	90
Mechanical efficiency of the generator [7]	$\eta_{mech,TG}$ [%]	99
Electrical efficiency of the generator [7]	$\eta_{mech,G}$ [%]	99
Heat transfer efficiency[1]	$\eta_{elek,G}$ [%]	97
Heat recovery efficiency[1]	σ_{rek} [%]	75
Throttling of the refrigerant in the after-burning chamber[1]	Δp_{RWC} [%]	1
Throttling the refrigerant in the fuel stack[1]	Δp_{FC} [%]	10
Relative heat loss in the stack[1]	$\Delta Q_{ukł}$ [%]	5
[1] Arbitrarily chosen		

In a fuel cell with internal reforming, three main reactions occur: a steam reforming reaction (Eq. (10)), fuel cell reaction (Eq. (11)) and water gas shift reaction (Eq. (12)).

$$CH_4 + 2H_2O \longrightarrow 4H_2 + CO_2 \tag{10}$$

$$2H_2 + O_2 \longrightarrow 2H_2O \tag{11}$$

$$CO + 2H_2O \Leftrightarrow CO_2 + H_2 \tag{12}$$

Combining Eq. (10) and Eq. (11) gives Eq. (13), which is the base for calculation of the anode gas composition.

$$CH_4 + O_2 \longrightarrow 2H_2O + CO_2 \tag{13}$$

A major assumption is the reformer inlet gas composition (fuel) – 100% methane. Firstly, the amount of hydrogen fed to the anode was calculated. That amount of hydrogen was used to calculate the quantity of methane. It is necessary to take into consideration the reformer and anode together, because these two parts affect each other. In the first step of calculation, the water shift reaction was not taken into consideration, so it was easy to evaluate the shares of the compounds (Table 3, *next page*).

Table 3 contains an artificial solution that reflects two out of three reactions. In the next step, the shift water reaction (Eq. (12)) was taken into consideration. The reaction does not proceed completely to the left or to the right, but to an equilibrium point, where both products and reactants remain. The equilibrium concentration is defined by Eq. (14), where K represents the equilibrium constant. The variable x represents the extent of the reaction to proceed to the right.

Tab 3. Spent fuel effluent calculation without shift reaction (for optimal point)

	FC inlet		Reforming / FC reaction	Reforming	FC outlet	
	[% mol]	[mol/s]	[mol/s]	[mol/s]	[mol/s]	[% mol]
Methane	100.0	20.98	–17.83	–3.15	0.00	0.0
Carbon monoxide	0.0	0.00	0.00	0.00	0.00	0.0
Carbon dioxide	0.0	0.00	17.83	3.15	20.98	33.3
Hydrogen	0.0	0.00	0.00	12.59	12.59	20.0
Water	0.0	0.00	35.66	–6.29	29.37	46.7
Sum	100.0	20.98	35.66	6.29	62.93	100.0

Constant K depends on the average fuel cell temperature and is described by Eq. (15).

$$K = \frac{[(CO_2)+x]\cdot[(H_2)+x]}{[(CO)-x]\cdot[(H_2O)-x]} \tag{14}$$

$$K = \exp\left(-2{,}4198 + 0{,}003855 \cdot T + \frac{2180{,}6}{T}\right) \tag{15}$$

The recast of Eq. (15) gives Eq. (16), which is the standard quadratic form of the square equation.

$$(1-K)x^2 + \{(CO_2) + (H_2) + K[(CO) + (H_2O)]\} \cdot$$
$$\cdot x + \{(CO_2)\cdot(H_2) - (CO)\cdot(H_2O)\cdot K\} = 0 \tag{16}$$

Eq. (16) usually gives two solutions and the one contained between –1 and 1 can be taken into consideration as the effect of the shift reaction in Table 4.

Tab. 4. Spent fuel effluent calculation with shift reaction (for optimal point)

	FC outlet without shift reaction		Effect of shift reaction	FC outlet	
	[% mol]	[mol/s]	[mol/s]	[mol/s]	[% mol]
Methane	0.0	0.00	0.00	0.00	0.0
Carbon monoxide	0.0	0.00	4.14	4.14	6.8
Carbon dioxide	33.3	20.98	–4.14	16.84	26.7
Hydrogen	20.0	12.59	–4.14	8.45	13.4
Water	46.7	29.37	4.14	33.51	53.2
Sum	100.0	62.93	0.00	62.93	100.0

Behind the fuel cell stack, there is an after-combustion chamber, which burns the hydrogen remaining after the reaction in the stack. As a rule, more fuel than necessary is used, as this allows the fuel cell to maintain the maximum efficiency. Behind the stack, the chemical composition of the working medium changes, and its temperature increases. For material reasons, this temperature should not be too high, as when it exceeds 1000°C, the turbine first stage blades need cooling, which decreases the turbine efficiency. On the other hand, increasing the inlet temperature leads to an increase in the efficiency of the entire cycle [7].

The heat flux Q_{FC} generated by the fuel cell is calculated from Eq. (17).

$$\dot{Q}_{FC} = W_{d,H2} \cdot \dot{m}_{pal} - N_{el,FC} \tag{17}$$

Part of this heat is lost to the environment, and another part is used in the reforming process. This fact is taken into account in Eq. (18). The reforming process consumes about 30% of the total heat generated in the fuel stack. The remaining part of the heat, which in this paper is referred to as the waste heat (Q_{odp}), is used for heating the working medium flowing through the fuel cell.

$$\dot{Q}_{odp} = \dot{Q}_{FC} - \dot{Q}_{reforming} \tag{18}$$

Behind the after-combustion chamber, there is a heat exchanger which heats the compressed air leaving the compressor. The assumed temperature at the turbine inlet is equal to $T_{2T} = 900$°C, although the effect of its change on system performance has been analysed. Like the compression, the expansion in the turbine is modelled as an irreversible adiabatic process, assuming some internal efficiency η_T of the machine. The final temperature of the conversion is given by Eq. (19) (taken from [7]).

$$T_{3T} = T_{2T} \cdot \left\{1 - \eta_T \cdot \left[1 - \left(\frac{1}{\pi_T}\right)^{\frac{K_T - 1}{K_T}}\right]\right\} \tag{19}$$

where κ_T is the adiabatic exponent, averaged for the expansion in the entire turbine. Since it depends on both temperature and pressure, its value was calculated in an iterative manner in the study. The pressure and temperature values at the turbine inlet and exit make the basis for calculating the specific enthalpy h and the turbine power output N_T (Eq. (20)). The power N_{spr} consumed by the compressor can be defined in the same way (Eq. (21)), while the power $N_{TG,el}$ of the gas turbine set is the difference between these quantities, corrected by mechanical and electric losses (Eq. (22)). In this case, $\eta_{e\text{-}mech,TG}$ is the electromechanical efficiency of the generator.

$$N_T = \dot{m}_{pow} \cdot (h_{3T} - h_{2T}) \tag{20}$$

$$N_{spr} = \dot{m}_{pow} \cdot (h_{1T} - h_0) \tag{21}$$

$$N_{TG,el} = N_T \cdot \eta_{e-mech,TG} - N_{spr} \quad (22)$$

The efficiency of the entire system is calculated by summing up the net electric powers reached by the two subsystems and dividing this sum by the flux of chemical energy delivered with the fuel (Eq. (23)).

$$\eta_{og} = \frac{N_{FC,netto} + N_{TG,el}}{\dot{m}_{CH4} \cdot W_d} \quad (23)$$

Part of the heat flux is used for reforming purposes, while the remaining part constitutes a loss in the case of a standalone fuel cell stack. The average temperature inside the fuel stack is the resulting value that depends on the fuel cell's efficiency and pressure. In the present case, this heat is used as a force driving the gas turbine set. As mentioned above, each of the two subsystems can be optimised individually. The parameters which are subject to control in the gas turbine set are the medium temperature at the turbine inlet and the compressor pressure ratio, while in the fuel cell, it is the efficiency which is the object of maximisation, with no attempt to optimise the current density. The first consequence of this situation is that the heat emission by the fuel cell is as low as possible, with the resultant relatively low temperature inside the fuel cell stack. The other effect is a relatively large working area of the stack. The pressure of the compressed air delivered to the fuel cell stack has been selected at a minimal level, which still allows the flow resistance through the system to be overcome. The turbine set was optimised with respect to the compressor pressure ratio. The effect of the air temperature at the turbine inlet on the compressor pressure ratio is shown in Fig. 6. Increasing the temperature leads to an increase of efficiency and the optimal pressure ratio values. The parameters finally obtained as a result of optimisation are collated in Table 5, while the system performance is presented in Table 6. The above analysis shows that combining the fuel cell stack with a gas turbine set has made it possible to increase the power output of the system by more than 1 MW, i.e. about 10%, with a simultaneous efficiency increase of several percent. It can be observed that two media leave the system: the air – point 3T, and the exhaust gas - point 7 (nomenclature as in Fig. 5 and Table 5). The air temperature is above 480°C, but the possible application of heat regeneration in the gas

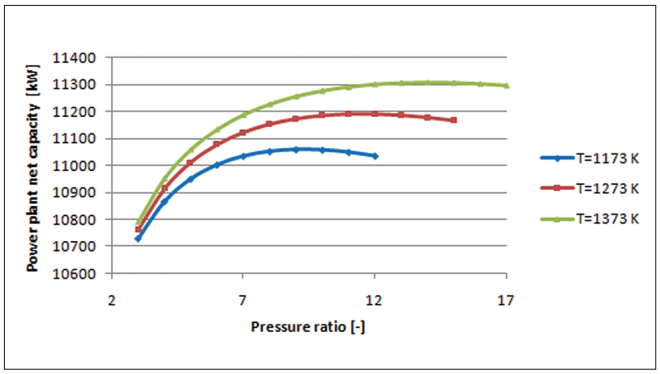

Fig. 6. The effect of compression in the compressor and the temperature of the medium before the turbine on the power of the hybrid system

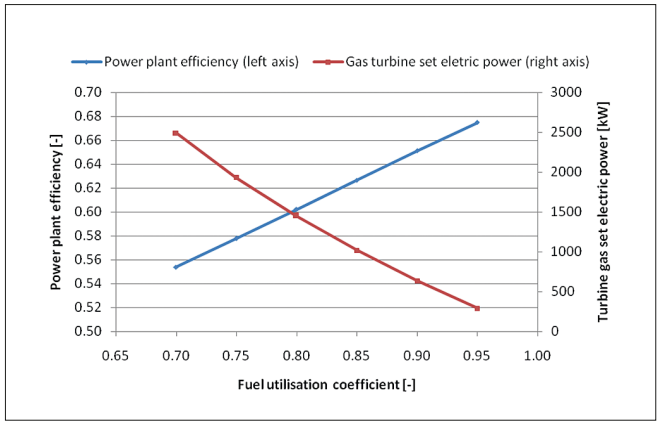

Fig 7. The influence of fuel utilisation coefficient on power plant efficiency and turbine gas set electric power(compression ratio = 9)

turbine set could worsen the heat transfer (lower temperature difference) and increase the temperature of the exhaust gas leaving the heat exchanger, which in the analysed case was equal to 254°C. Therefore, the most effective utilisation of this waste heat seems to be to expand the power plant by a heating part.

The fuel utilisation coefficient has an impact on the performance of the hybrid system (Fig 7). The more fuel reacts in the fuel cell, the less electricity is generated in the gas turbine set. On the other hand, when the fuel utilisation coefficient is close to 1, the overall hybrid system efficiency reaches the highest value (over 68%). These two phenomena take place because the SOFC converts chemical energy more effectively than the gas turbine does.

Tab. 5. Parameters of the factor at characteristic points of the indirect hybrid system (Tab. 5 → continued next page)

Fuel cell stack									
Point	0	1	2	3	4	5	6	7	P
Factor (mass shares)	Air: N_2 75.6%, O_2 23.2%, Ar 1.3%, H_2O 0.9%			CO 7.84%, CO_2 50.15%, H_2 1.15%, H_2O 40.85%	N_2 86.89%, O_2 10.65%, Ar 1.46%, H_2O 1.00%	N_2 71.99%, O_2 7.26%, Ar 1.21%, CO 1.34%, CO_2 8.60%, H_2O 9.60%			CH_4
Temperature [°C]	20	62.2	450.0	872.4		1029.7	579.3	254.6	20
Pressure [MPa]	0.102	0.15	0.143	0.128		0.128	0.122	0.116	0.65
Mass stream [kg/s]	8.212			1.478	7.142	8.620			0.35

Tab. 5. Parameters of the factor at characteristic points of the indirect hybrid system

Gas turbine set				
Point	0	1T	2T	3T
Factor (mass shares)	Air: N_2 75.6%, O_2 23.2%, Ar 1.3%, H_2O 0.9%			
Temperature [°C]	20.0	341.0	900.	485.0
Pressure [MPa]	0.102	1.101	0.962	0.102
Mass stream [kg/s]	7,986			

Tab. 6. The most important parameters of an indirect hybrid system

Quantity	Symbol [unit]	Value
Current density	i [mA/cm²]	120
Fan compression ratio	π_{went} [–]	1.48
Compressor's optimal compression ratio	π_s [–]	9
Electrical power of a gas turbine set	$N_{el,TG}$ [kW]	1058
Net power of the unit	$N_{ukł,netto}$ [kW]	11058
Overall efficiency	η_{Fog} [%]	62.6%

DIRECT HYBRID SYSTEM

A distinctive feature of the direct hybrid system is that the pressure in the fuel cell stack depends on the pressure ratio in the gas turbine set compressor. From the point of view of the turbine set, this is a system with heat regeneration in which the fuel cell stack plays the role of a combustion chamber (Fig. 8). When analysing the schematic diagram, we can see the advantage of this system over the previous one, which is the presence of only one heat exchanger playing the role of a regenerative air heater. Moreover, there is no additional blower.

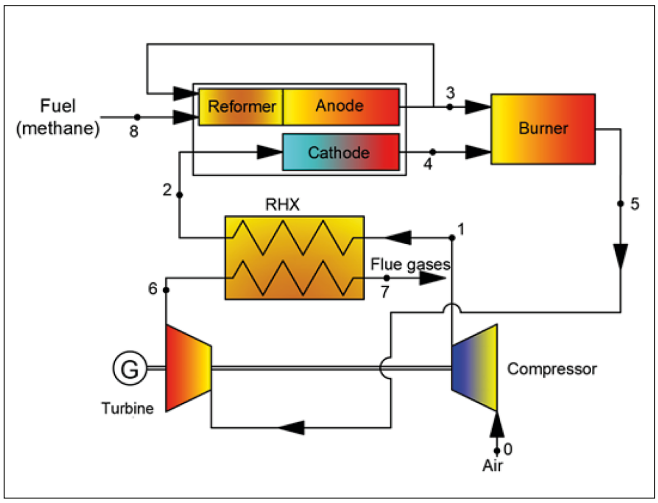

Fig. 8. Schematic diagram of a direct hybrid system with marked characteristic points (RHX – Regenerative Heat Exchanger)

The regenerative heat exchanger plays a key role and only the compact heat exchangers with passive techniques of the heat transfer augmentation are promoted. Noteworthy in this case are the modern, highly efficient constructions dedicated to the gas/vapour micro-CHP units – for example, heat exchangers with minichannels of cylindrical construction [3] and plate ones [16, 28]. The stainless steel radial recuperators [16] or the ceramic plate microchannel heat exchangers [14] are also considered. However, the most promising seem to be the heat exchangers with the micro-jets technology – intensive experimental [29] and numerical [11, 12] investigations of their development are being conducted at the moment. The direct hybrid system has one degree of freedom less than the indirect system. In this system, the quantities to be optimised are the compressor pressure ratio and the fuel cell stack current density. However, also in this case, the temperatures at the fuel cell and after-combustion chamber exits are to be taken into account, as they must not be too high for material reasons and possible turbine stage cooling problems. The calculation analysis is very similar to that performed for the previous variant. The pressure effect on the power output and efficiency is shown in Figs. 9 and 10. The maximum power output of the system corresponds to about 0.5 MPa, while the maximum efficiency is reached by the system at a pressure of 0.8 MPa. Both curves, especially the efficiency characteristic, are relatively flat, which has made it possible to select the working point as a compromise between the two indicators. It is noteworthy that the optimal pressure ratio is close to typical values of a gas turbine set with heat regeneration. Eventually, the current density has been left at the same level as in the previous variant (Table 7). The analysis has revealed that the direct variant makes it possible to reach much higher efficiency than the indirect variant. In the direct variant, the turbine set reached the power output of nearly 1.6 MW, which is 50% more than in the indirect variant. The analysis included checking the effect of the compressor discharge pressure on the temperatures at the turbine inlet and exit (points 5 and 7). It turns out that, above some level, the temperature of the medium leaving the system practically does not change, as can be seen in Fig. 11. However, in absolute values, it is nearly 500°C, which suggests possible utilisation of this waste heat flow. An option proposed in [25] is to install a waste heat boiler which would be used to meet heating needs. Another possibility is to expand the hybrid system

a steam turbine. The analyses performed suggest that when a proper working medium is selected, the efficiency of such a triple hybrid system would increase to 78%, and the power output to about 900 kW.

In the case of the direct hybrid system, fuel utilisation close to 1 is not favourable for the performance of the gas turbine (Fig. 12), because of the low turbine inlet temperature (Fig. 13), which strongly depends on the fuel utilisation in the SOFC.

The cycle calculations were the basis for designing selected flow devices for the hybrid system, including a 1592 kW gas turbine set (Fig. 14), which consists of a 7-stage axial compressor and a 5-stage turbine. The designed turbine set is in a single-shaft arrangement and its nominal speed is 13,800 rpm. The basic component of the system is the fuel cell stack. It consists of individual fuel cells of tubular shape, the inner and outer parts of which play the roles of anode and cathode, respectively. Due to the large power of the stack, its working area is also large, so a decision was made to group the fuel cells into sets of 16 cylinders (detailed data in Table 8). One selected set is shown in Fig. 16, while for comparison purposes, Fig. 15 shows the regenerative air/exhaust gas heat exchanger.

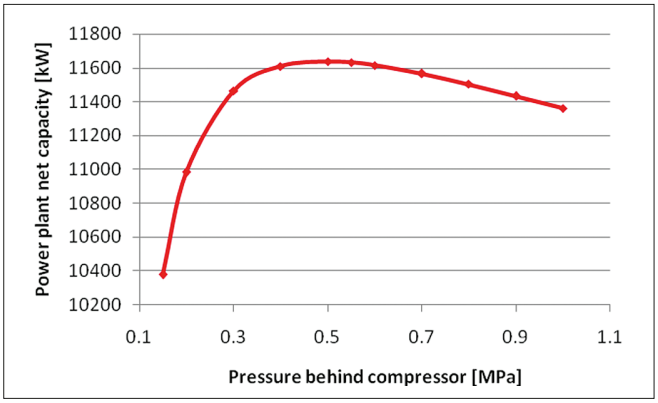

Fig. 9. The effect of pressure behind the compressor on the power of the hybrid system

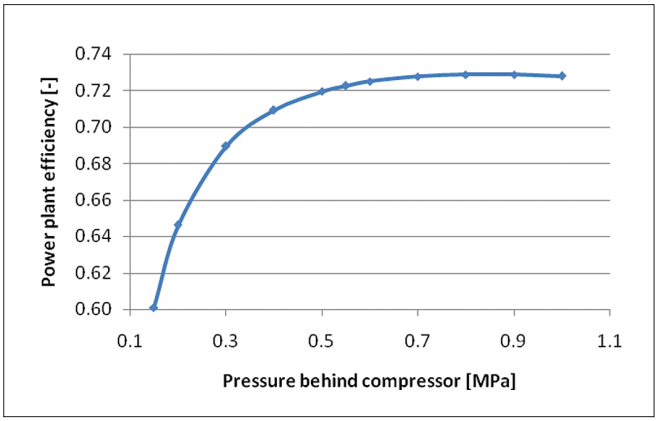

Fig. 10. The effect of pressure behind the compressor on the efficiency of the hybrid system

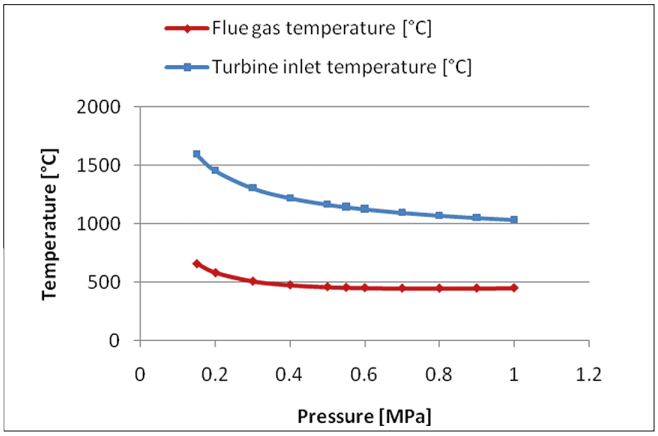

Fig. 11. The influence of pressure behind the compressor on the temperature of the medium at characteristic points of circulation

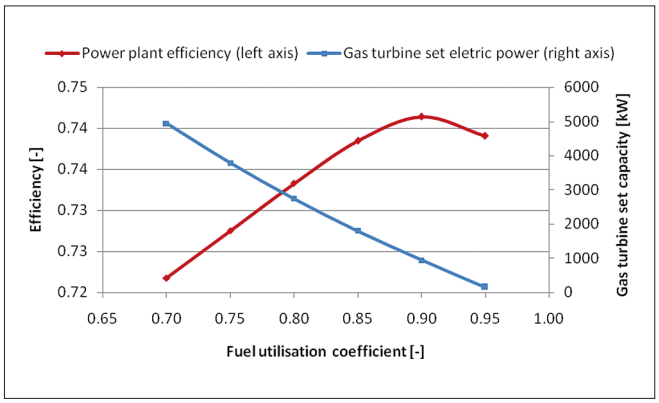

Fig. 12. The influence of the fuel utilisation coefficient on the efficiency of the hybrid system and gas turbine set electric power (compression ratio=6.5)

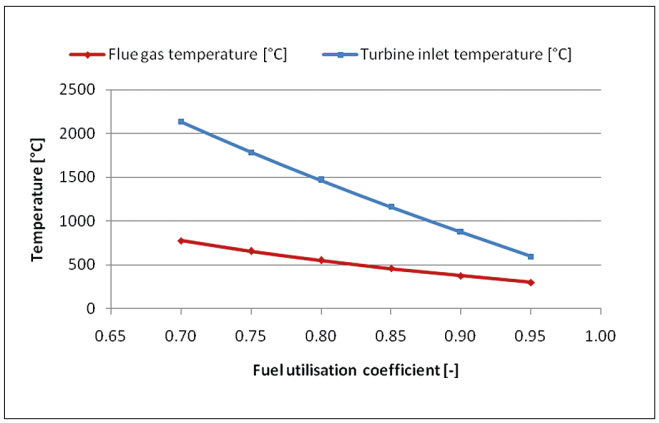

Fig. 13. The influence of the fuel utilisation coefficient on the temperature of the medium at characteristic points of circulation (compression ratio=6.5)

Tab. 7. The most important quantities describing the direct hybrid system

Quantity	Symbol [unit]	Value
Current density	i [mA/cm^2]	120
Fan compression ratio	π_s [–]	6.5
Compressor's optimal compression ratio	σ [mW/cm^2]	96
Electrical power of a gas turbine set	$N_{el,TG}$ [kW]	1592
Net power of the unit	$N_{ukl,netto}$ [kW]	11592
Overall efficiency	η_{og} [%]	72.7

Tab. 8. The most important quantities describing the fuel stack

Quantity	Symbol [unit]	Value
The internal diameter of the cell	D_w [mm]	26.08
The average diameter of the cell	$D_{śr}$ [mm]	28.04
The total working surface of the stack	A_s [m²]	10417
Number of individual links	n	65694
Number of cells in one set	k	3734
Number of sets	m	16

Tab. 9. Assumptions for economic analysis

Quantity	Symbol [unit]	Value
Power plant work time [h]	t_p	7500
Capacity utilisation factor [-]	SWM	0.8
The lifetime of the cell stack [hour]	$t_{życia}$	60000
Emission of CO_2 [kg/MWh]	$\dot{m}_{CO2}$	208.4
Emission of CO [kg/MWh]	$\dot{m}_{CO}$	32.4
Unit cost of a fuel cell [$/kW]	k_{FC}	1500
Unit cost of a gas turbine set [$/kW]	k_{TG}	698
The wholesale price of electricity [$/MWh]	k_{elek}	44

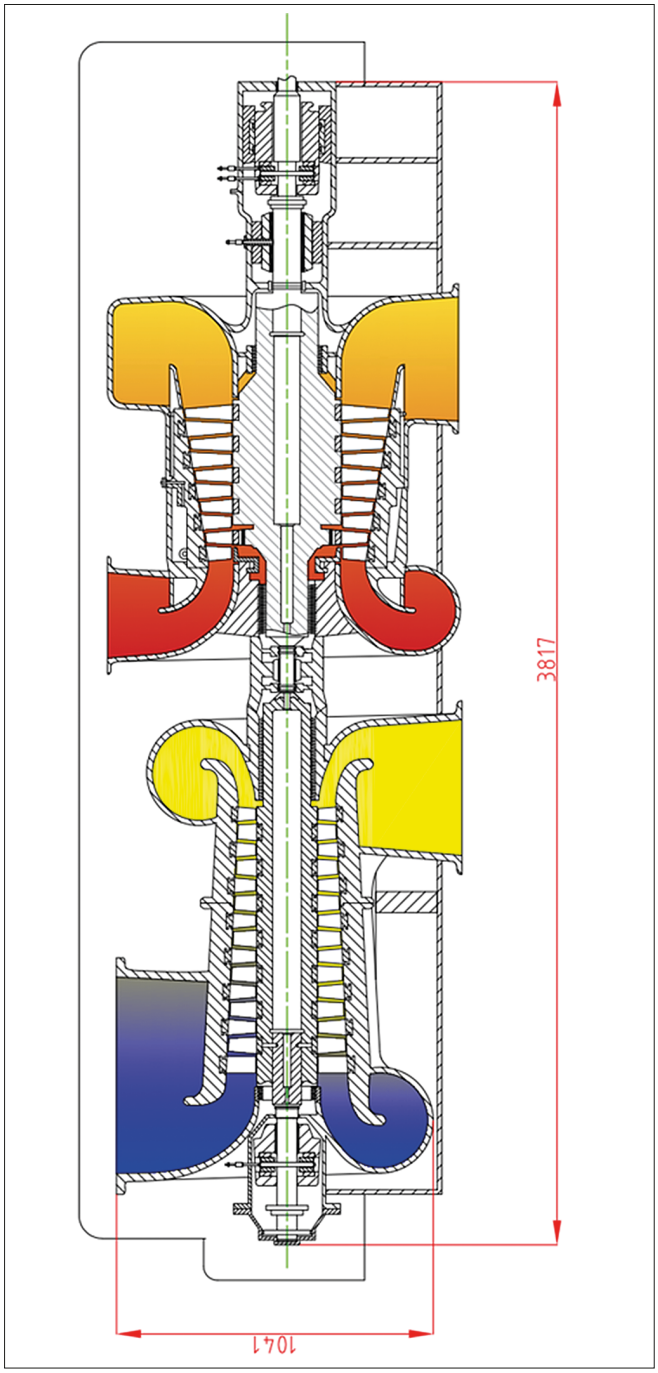

Fig. 14. Designed gas turbine set (dimensions in mm)

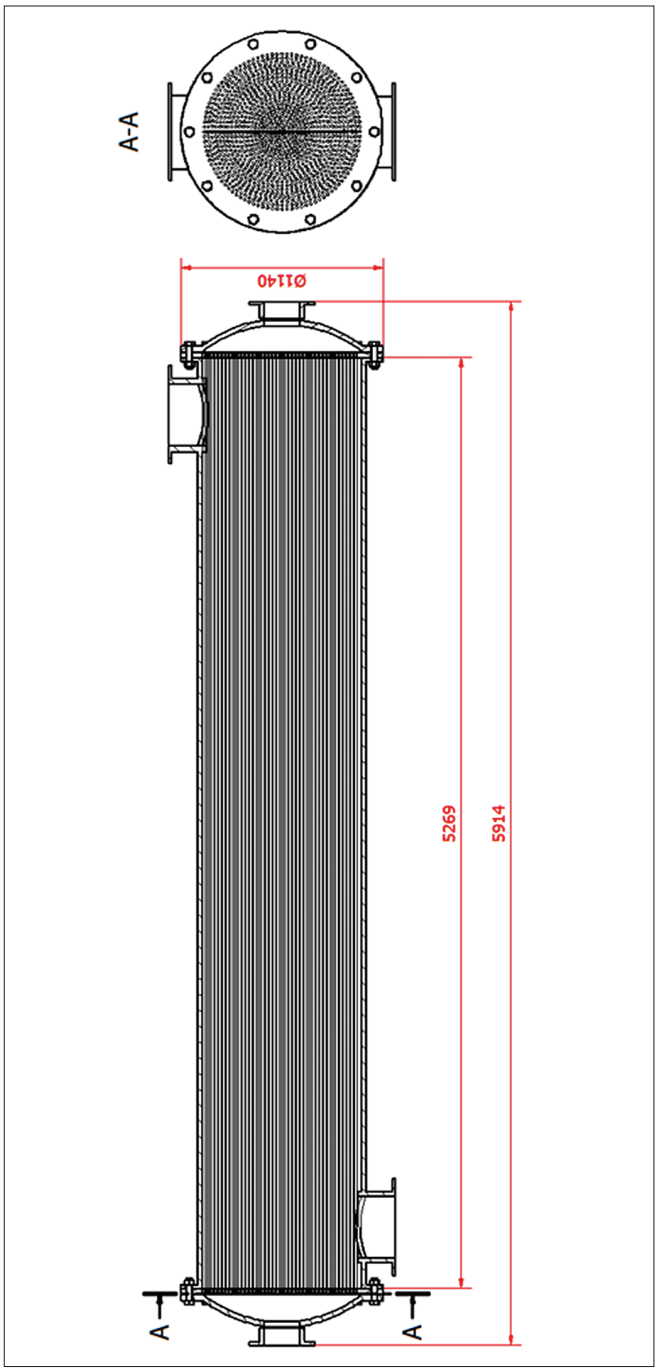

Fig. 15. Designed regenerative heat exchanger (dimensions in mm)

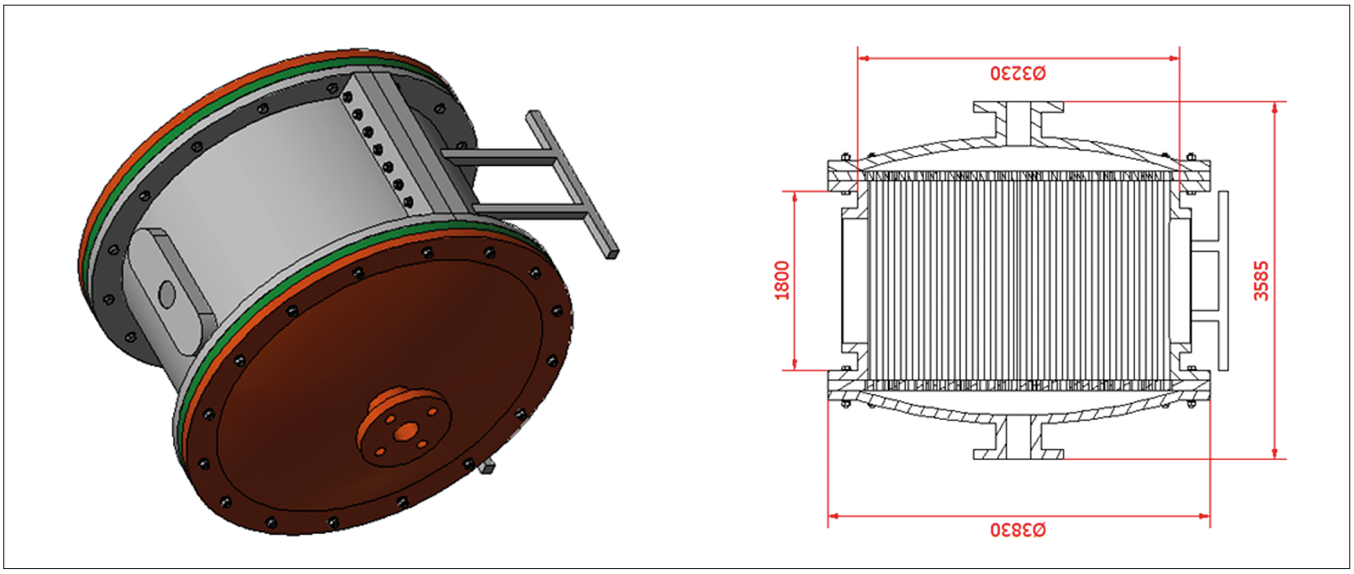

Fig. 16. Designed fuel cell stack (dimensions in mm)

ECONOMIC ANALYSIS

Based on certain assumptions concerning: the operating time of the power plant, the capacity utilisation factor, expected lifetime of the fuel cell, etc. (Table 9), the profitability analysis was performed for the designed hybrid system when in operation in Poland. All investment expenditures were booked by default as for year 0 of investment existence. The discounted cash flows and the updated net value of the investment are shown in Fig. 17. The payback period of the investment, amounting to 17 years, is longer than the lifetime of the high-temperature fuel cell, which makes constructing such a power plant unprofitable. The aspects which considerably affect its profitability include the price of electricity, the unit cost of the fuel cell, and the price of fuel (natural gas). Fig. 18 shows the effect of changes in the values of the above quantities on the payback period (and, consequently, the profitability of the investment). It turns out that it is the price of electricity which affects the payback period most: increasing this price by 20% results in a decrease of the discounted payback period by about 33%. Since mid-2018, an upward trend can be observed in electricity prices in long-term contracts at the Polish Power Exchange. If this trend continues, the hybrid system may turn out to be profitable within a few years.

The principal obstacle to the hybrid system's successful commercialisation is the high cost of the SOFC. In marine applications the installed capital cost of SOFC–GT systems should be compared with current marine diesel and marine gas turbine power plants. The installed capital cost of diesel engines varies from 125 to 300 $/kW and that of gas turbines is in the range of 300–600 $/kW, whereas the installed capital cost of the SOFC is 1000–1500 $/kW [30].

CONCLUSIONS

The presented hybrid system is a thermodynamic combination of two power systems: a gas turbine and fuel cell (stack). Linking these systems together makes it possible to generate much more useful energy than in the case of individual operation of these devices at the same fuel consumption. The paper presents two variants of gas turbine/fuel cell linkage. The examined issues included the

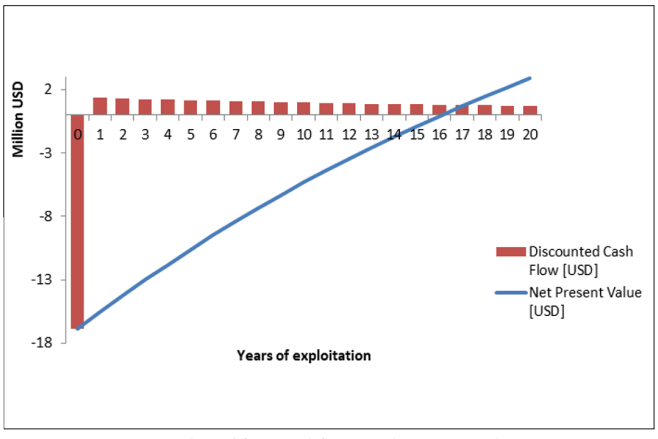

Fig. 17. Value of financial flows and NPV over the years of the designed power plant's operation

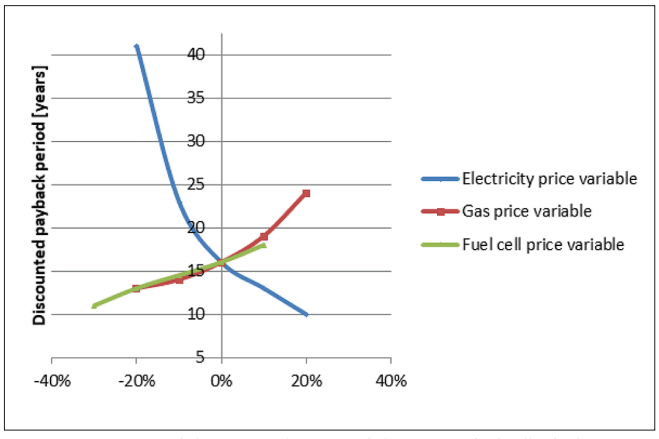

Fig. 18. Impact of changes in the price of electricity / fuel cell / fuel price for the discounted investment return period

effect of the working pressure in the fuel cell stack and the current density on the performance of the entire system. The analysis has revealed that the direct variant is more favourable, due to the higher efficiency and slightly simpler structure (the absence of an air blower for the fuel cell). At present, this type of hybrid power plant is unprofitable due to the high production cost of fuel cells, although the increase in electricity prices at the Polish Power Exchange in 2018 and 2019 shows that this technology may turn out to be economically profitable within a few years. Moreover, the efficiency, which is higher than that of all other known power technologies in operation, provides an incentive for further attempts to develop hybrid systems on a smaller or larger scale. Lower emission of harmful compounds than conventional diesel engines, and high efficiency above 60%, makes the hybrid connection of the fuel cell with the gas turbine an excellent starting point for activities aimed at using these systems for the propulsion of ships and other mobile devices. The relatively large dimensions of both the heat exchanger and the fuel stack can present serious installation problems. However, these are the values resulting from the assumed 10 MW electric capacity. In the case of reduced power, the dimensions will be reduced, which will facilitate their use on ships.

REFERENCES

1. Badami M., Chicco G., Portoraro A., Romaniello M. (2018): *Micro-multigeneration prospects for residential applications in Italy*. Energy Conversion and Management,Vol. 166, 23–36, https://doi.org/10.1016/j.enconman.2018.04.004.

2. Cieśliński J., Kaczmarczyk T., Dawidowicz B. (2017): *Performance of the PEM fuel cell module. Part 2. Effect of excess ratio and stack temperature*. Journal of Power Technologies, Vol. 97(3), 246-251.

3. Chordia, L. (2019): *High temperature heat exchanger design and fabrication for systems with large pressure differentials*. Final Scientific/Technical Report 2017. Available online: www.osti.gov/servlets/purl/1349235 (accessed: 26.4.2019).

4. Ferrari M. L., Damo U. M., Turan A., Sanchez D. (2017): *Hybrid Systems Based on Solid Oxide Fuel Cells: Modelling and Design*, Wiley & Sons Ltd.

5. Seddiek I. S., Elgohary M. M., Ammar N. R. (2015): *The hydrogen-fuelled internal combustion engines for marine applications with a case study*. Brodogradnja/Shipbilding, Vol. 66(1), 23–38.

6. ISO-2314:2009 Gas turbines – Acceptance tests.

7. Kosowski K., Domachowski Z., Próchnicki W., Kosowski A., Stępień R., Piwowarski M., Włodarski W., Ghaemi M., Tucki K., Gardzilewicz A., Lampart P., Głuch J., Łuniewicz B., Szyrejko C., Obrzut D., Banaszkiewicz M., Topolski J., Kietliński K., Ferdyn Z. (2007): *Steam and gas turbines. Power plants, France; Switzerland; UK; Poland*: ALSTOM. ISBN 978-83-925959-1-5.

8. Kosowski K., Piwowarski M., Stepien R., Włodarski W. (2018): *Design and investigations of the ethanol microturbine*. Archives of Thermodynamics, Vol. 39, 41–54. doi:10.1515/aoter-2018-0011.

9. Kosowski K., Tucki K., Piwowarski M., Stępień R., Orynycz O., Włodarski W., Bączyk A. (2019): *Thermodynamic cycle concepts for high-efficiency power plants. Part A: Public power plants 60+*. Sustainability, Vol. 11(2), 554–565. doi: 10.3390/su11020554.

10. Kosowski K., Tucki K., Piwowarski M., Stępień R., Orynycz O., Włodarski W. (2019): *Thermodynamic cycle concepts for high-efficiency power plants. Part B: Prosumer and distributed power industry*. Sustainability, Vol. 11, 26–47. doi:10.3390/su11092647.

11. Kura T., Fornalik-Wajs E., Wajs J., Kenjeres S. (2018): *Turbulence models impact on the flow and thermal analyses of jet impingement*. MATEC Web of Conferences, 2018, Vol. 240, 01016, doi: 10.1051/matecconf/201824001016.

12. Kura T., Fornalik-Wajs E., Wajs J. (2018): *Thermal and hydraulic phenomena in boundary layer of minijets impingement on curved surfaces*. Archives of Thermodynamics, Vol. 39(1), 147–166.

13. Lara-Curzio E., Maziasz P. J., Pint B. A., Stewart M., Hamrin D., Lipovich N., DeMore D. (2002); *Test facility for screening and evaluating candidate materials for advanced microturbine recuperators*, Proc. ASME Turbo Expo 2002, 3-6 June 2002 Amsterdam, GT-2002-30581.

14. Lewinsohn C. A., Wilson M. A., Fellows J. R., Anderson H. S. (2012); *Fabrication and joining of ceramic compact heat exchangers for process integration*. International Journal of Applied Ceramic Technology, Vol. 9(4), 700–711.

15. Mikielewicz J., Piwowarski M., Kosowski K., *Design analysis of turbines for cogenerating micro-power plant working in accordance with organic Rankine's cycle*. Polish Maritime Research (Special issue) (2009) 34-38. doi:10.2478/v10012-008-0042 4.

16. Mikielewicz J., Wajs J. (2017): *Possibilities of heat transfer augmentation in heat exchangers with minichannels for marine applications*. Polish Maritime Research, Vol. 24, Special Issue S1, 133–140, doi: 10.1515/pomr-2017-0031.

17. Ministerstwo Energii (2018): *Polityka Energetyczna Polski do 2040 roku (PEP 2040)*, Warszawa (in Polish, version from 13.11.2018).

18. Mitsubishi Heavy Industries Press Information (20.09.2013): MHI Achieves World's First 4,000-Hour Continuous Operation of Pressurized SOFC-MGT Hybrid Power Generation System, www.mhi.com (accessed: 21.10.2018).

19. National Institute of Standards and Technology, Reference Fluid Thermodynamic and Transport Properties Database (REFPROP), ver. 9.0.

20. O'Hayre R., Suk-Won C., Colella W., Prinz F. B. (2016): *Fuel Cell Fundamentals*, John Wiley & Sons, Hoboken, New Jersey.

21. Piwowarski M., Kosowski K. (2014): *Design analysis of combined gas-vapour micro power plant with 30 kW air turbine*. Polish Journal of Environmental Studies, Vol. 23, 1397–1401.

22. Polskie Sieci Elektroenergetyczne (2018): *Zestawienie danych ilościowych dotyczących funkcjonowania KSE w 2017 roku*, Konstancin-Jeziorna, in Polish.

23. Stępniak D., Piwowarski M. (2014): *Analyzing selection of low-temperature medium for cogeneration micro power plant*. Polish Journal of Environmental Studies, Vol. 23(4), 1417–1421.

24. Świrski K. (26.11.2018): *PEP 2040 – czy rozwiązuje wszystkie problemy?* Szersza analiza, www.cire.pl (in Polish, accessed: 12.03.2019).

25. Toyota Motor Corporation (26.04.2017): *Toyota Starts Trial of a Hybrid Power Generation System Combining Fuel Cell Technology with Micro Gas Turbines at Motomachi Plant*. www.newsroom.toyota.cp.jp, (accessed: 21.10.2018).

26. U.S. Department of Energy (2004): *Fuel Cell Handbook*, EG&G Technical Services, Margatown, West Virginia.

27. Ustawa z dnia 20 maja 2016 r. o inwestycjach w zakresie elektrowni wiatrowych, Dz.U. 2016 poz. 961, http://prawo.sejm.gov.pl (in Polish, accessed: 7.10.2018).

28. Wajs J., Mikielewicz D., Fornalik-Wajs E. (2016): *Thermal performance of a prototype plate heat exchanger with minichannels under boiling conditions*. Journal of Physics Conference Series, Vol. 745, 032063.

29. Wajs J., Mikielewicz D., Fornalik-Wajs E., Bajor M. (2019): *High performance tubular heat exchanger with minijet heat transfer enhancement*. Heat Transfer Engineering, Vol. 40(9–10), 772–783.

30. Welaya Y. M. A., Morsy El-Gohary M., Ammar N. R. (2011): *A Comparison Between Fuel Cells and Other Alternatives For Marine Electric Power Generation*. International Journal of Naval Architecture and Ocean Engineering (JNAOE), Korea, SNAK, Vol. 3, 141–149.

31. Welaya Y. M. A., Mosleh M., Ammar N. R. (2013): *Thermodynamic analysis of a combined gas turbine power plant with a solid oxide fuel cell for marine applications*. Int. J. Naval Archit. Ocean Eng., Vol. 5, 404–413.

32. Welaya Y., Mosleh M., Ammar N. (2013): *Thermodynamic analysis of combined gas turbine power plant with a solid oxide fuel cell for marine applications*. International Journal of Naval Architecture and Ocean Engineering, Vol. 5(4), 529–545.

33. Włodarski W. (2018): *Experimental investigations and simulations of the microturbine unit with permanent magnet generator*. Energy, Vol. 158, 59–71. doi:10.1016/j.energy.2018.05.199.

34. Włodarski W. (2019): *Control of a vapour microturbine set in cogeneration applications*. ISA Transactions, 2019, doi.org/10.1016/j.isatra.2019.04.028.

35. Włodarski W. (2019): *A model development and experimental verification for a vapour microturbine with a permanent magnet synchronous generator*. Applied Energy, Vol. 252, doi.org/10.1016/j.apenergy.2019.113430.

36. Würsig G. (2017): Zero Emissions, in: *Ferry and Ro-ro update*, DNV-GL, Maritime Communications, www.dnvgl.com.

CONTACT WITH THE AUTHORS

Tomasz Kwaśniewski
e-mail: tomkwasn@gmail.com
Gdańsk University of Technology
11/12 Gabriela Narutowicza Street, 80-233 Gdańsk
Poland

Marian Piwowarski
e-mail: marian.piwowarski@pg.edu.pl
Gdańsk University of Technology
11/12 Gabriela Narutowicza Street, 80-233 Gdańsk
Poland